ORIGINAL ARTICLE

10.2478/AMB-2026-0007

SPATIAL DYNAMICS OF CUPRIZONE-INDUCED MYELIN LOSS AND RECOVERY IN THE MOUSE CORPUS CALLOSUM

L. Gaydarski[1], K. Petrova[1], G.P. Georgiev[2], B. Landzhov[1]

[1]Department of Anatomy, Histology and Embryology, Medical University – Sofia, Bulgaria
[2]Department of Orthopedics and Traumatology, University Hospital "Tsaritsa Yoanna-ISUL", Medical University – Sofia, Bulgaria

Abstract. Background: *The corpus callosum (CC) is a principal site of white matter pathology in multiple sclerosis and a common target for experimental demyelination–remyelination studies. The cuprizone model produces reproducible oligodendrocyte loss and myelin depletion, enabling controlled analysis of regional myelin dynamics.* ***Materials and Methods:*** *Thirty male C57BL/6 mice (8 weeks old) were randomized to control (n = 10), demyelination (0.2% cuprizone, 5 weeks; n = 10), or remyelination (0.2% cuprizone, 5 weeks, followed by 5 weeks of recovery; n = 10) groups. Coronal sections spanning bregma +0.98 to +0.02 were stained with Luxol Fast Blue (LFB) and the CC was subdivided into medial (CC-M) and lateral (CC-L) regions. Every fifth section was analyzed (15 sections per brain), generating 150 quantified fields per subregion. LFB intensity was quantified and group comparisons were performed using the Kruskal–Wallis test with Dunn's post hoc analysis (α = 0.05).* ***Results:*** *Cuprizone exposure produced marked, regionally heterogeneous demyelination: morphologically, LFB signal was greatly diminished with pallor, thinning of the myelin band and focal signal loss, changes that were more pronounced in CC-L than CC-M. Quantitatively, mean whole-CC LFB intensity fell significantly after cuprizone (Kruskal–Wallis $p < 0.0001$); post hoc tests showed control vs demyelination ($p < 0.0001$) and demyelination vs remyelination ($p < 0.0001$), whereas control vs remyelination did not differ significantly ($p > 0.05$). Subregional analyses mirrored the overall pattern ($p < 0.0001$ for CC-M and CC-L), and revealed a significant medio-lateral difference during demyelination with CC-L < CC-M ($p = 0.03$). After five weeks of recovery, LFB intensity increased in both subregions but myelin bands remained thinner and more heterogeneous than in controls.* ***Conclusions:*** *Five weeks of cuprizone elicited robust, spatially selective CC demyelination with greater lateral vulnerability; toxin withdrawal yielded substantial but structurally incomplete remyelination. These results emphasize the need for region-specific, multimodal assessment when evaluating remyelination and support targeting both OPC differentiation and mechanisms that improve myelin maturation and debris clearance in therapeutic strategies.*

Key words: *cuprizone, demyelination, remyelination, luxol fast blue, corpus callosum*

Corresponding author: *Lyubomir Gaydarski, MD, Department of Anatomy, Histology and Embryology, Medical University – Sofia, 2 Zdrave str, Sofia 1431, Bulgaria, tel: +359885037178, email: lgaidarsky@gmail.com*

ORCID: *0000-0003-4774-6507*

Received: *11 January 2026;* ***Accepted:*** *19 January 2026*

INTRODUCTION

Multiple sclerosis (MS) is characterized by the formation of multifocal demyelinating lesions throughout the central nervous system (CNS), with the corpus callosum (CC) being among the most frequently affected white matter structures [1, 2]. Owing to its size, clear anatomical boundaries, and high vulnerability to myelin loss, the CC has become a principal target in experimental studies investigating mechanisms of white matter injury and repair [3]. One of the most widely used experimental approaches to model CC demyelination is dietary administration of cuprizone, a copper-chelating neurotoxin that induces robust and reproducible oligodendrocyte loss and demyelination in rodents [4].

Several experimental models are available for studying demyelination, including experimental autoimmune encephalomyelitis (EAE), Theiler's murine encephalomyelitis virus (TMEV), lysophosphatidylcholine (LPC/lysolecithin), and cuprizone [4, 5]. Immune-mediated and viral models, such as EAE and TMEV, involve pronounced inflammatory components that introduce biological variability and complicate the analysis of CNS-intrinsic mechanisms of myelin damage and repair [6]. In contrast, toxin-based models, particularly the cuprizone model, induce demyelination primarily through metabolic and oxidative stress in oligodendrocytes and are largely independent of peripheral immune activation [7, 8]. Classically the cuprizone model is induced by cuprizone-enriched pallets in the mice chow [4, 5]. However, there are described variations of the model in the literature [9]. Acute cuprizone exposure results in consistent and regionally defined demyelination within 4–6 weeks, accompanied by microglial and astrocytic activation and relatively limited axonal damage [5, 10], while exerting minimal effects on the peripheral nervous system [7]. Prolonged administration leads to chronic demyelination and delayed remyelination, thereby enabling the study of both sustained injury and endogenous repair processes [5, 11]. Collectively, these properties render the cuprizone model particularly suitable for controlled investigations of CNS myelin dynamics [5, 7, 11].

The aim of the present study was to evaluate morphological changes in the mouse CC induced by cuprizone-mediated demyelination and during subsequent remyelination. Using coronal sections between bregma +0.98 and +0.02, the CC was subdivided into medial and lateral subregions in order to visualize and describe myelin quality and to compare region-specific effects of cuprizone on myelin integrity.

MATERIALS AND METHODS

Thirty male C57BL/6 mice (8 weeks old) were obtained from the vivarium of the Faculty of Medicine, Medical University – Sofia, Bulgaria. Animals were randomly allocated to three experimental groups (n = 10 per group): (1) control – maintained on standard chow for the duration of the study; (2) demyelination – subjected to a 5-week cuprizone regimen (0.2%); and (3) remyelination – subjected to the same 5-week 0.2% cuprizone exposure, followed by a 5-week recovery period on standard chow without cuprizone. Throughout the experiment mice were housed under controlled conditions (ambient temperature 22 ± 3 °C, relative humidity ≈ 30%) on a 12-hour light/12-hour dark cycle; all procedures were carried out during the light phase.

Demyelination was induced using the established cuprizone protocol (Landzhov). Cuprizone (CAS 370-81-0; Sigma-Aldrich, Vienna, Austria) was provided ad libitum at a final concentration of 0.2% in the drinking water for five weeks. After weeks cuprizone was withdrawn and animals in the remyelination group received plain drinking water for an additional five weeks to permit spontaneous remyelination. Control mice received unmodified drinking water throughout the whole experiment. All experimental procedures complied with Directive 2010/63/EU on the protection of animals used for scientific purposes and were approved by the Bulgarian Food Safety Agency (Approval Protocol No. 416/19.12.2024).

For tissue collection, animals were anesthetized by intraperitoneal injection of thiopental sodium (30 mg/kg; Sigma-Aldrich Chemie GmbH, Taufkirchen, Germany) and transcardially perfused with 4% paraformaldehyde in 0.1 M phosphate-buffered saline (pH 7.4; Merck Catalogue No. 1465920006). Brains (n = 30; 10 per group) were removed and post-fixed in the same fixative for 24 hours, rinsed, dehydrated through graded alcohols, cleared, and embedded in paraffin (Merck Catalogue No. 1071511000). Serial coronal sections (6 μm) spanning bregma +0.98 to +0.02, referenced to the atlas of Paxinos and Franklin [Paxinos], were cut on a Leica RM 2155 microtome (Wetzlar, Germany) for subsequent histological analysis.

Sections were mounted on gelatin-coated glass slides, then deparaffinized and rehydrated through graded alcohols to 95% ethanol (Merck Catalogue No. 1009835000). Myelin was visualized by incubating the sections in 0.01% Luxol Fast Blue solution (CAS L0294; Sigma-Aldrich, Vienna, Austria) for 2 hours at 58 °C. Excess stain was removed by differentiation in 0.05% lithium carbonate (CAS

255823; Sigma-Aldrich, Vienna, Austria), followed by counterstaining with cresyl violet (CAS 41830-80-2; Sigma-Aldrich, Vienna, Austria). After that air-drying sections were permanently mounted using Entellan (Merck Catalogue No. 1079600500). For each brain, every fifth coronal section within the bregma range 0.98–0.02 was analyzed and digitally recorded using an Olympus CX21 light microscope equipped with an Olympus C5050Z camera (Olympus Optical Co., Ltd., Tokyo, Japan) at 100× magnification.

All statistical analyses and graphical outputs were generated using GraphPad Prism (version 10.6.1) and IBM SPSS Statistics (version 28.0.0.1). Differences among experimental groups were evaluated using the non-parametric Kruskal–Wallis test. When a significant overall effect was detected, pairwise comparisons were performed using Dunn's post hoc test. A threshold of $p \leq 0.05$ was applied to define statistical significance. The CC was subdivided into medial (CC-M) and lateral (CC-L) regions for analysis, as illustrated in Figure 1. Each experimental group consisted of ten animals; from each group, 15 histological sections were analyzed, yielding a total of 150 quantified fields for CC-L and 150 for CC-M.

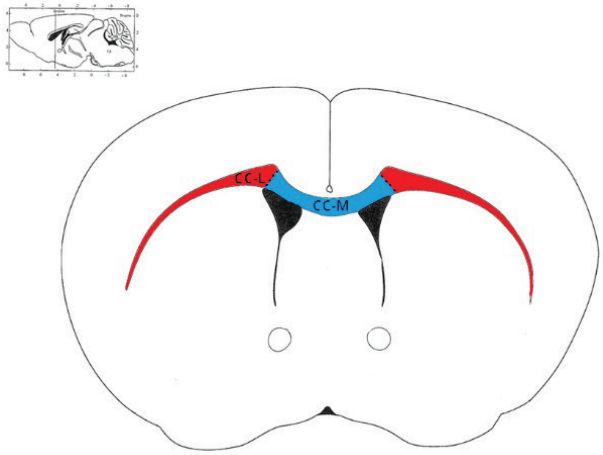

Fig. 1. Schematic coronal section of the mouse brain showing the regions of the corpus callosum selected for histological quantification. The medial corpus callosum (CC-M, blue) and lateral corpus callosum (CC-L, red) are highlighted as the regions of interest. The figure was adapted from the mouse brain atlas of Paxinos and Franklin [12]

RESULTS

The LFB staining of coronal sections demonstrated clear, region- and group-dependent alterations in myelin within the CC (Fig. 2). Morphologically, control animals displayed dense, homogeneous LFB labeling in both the CC-M (Fig. 1A) and CC-L (Fig. 2B) subregions, consistent with compact, well-preserved myelin sheaths. After five weeks of cuprizone administration, LFB signal was markedly reduced: demyelinated animals showed pallor and thinning of the myelin band with areas of near-complete signal loss and tissue rarefaction. These changes were evident in both subregions but were more pronounced in the CC-L (Fig. 2D), whereas the CC-M (Fig. 2C) exhibited patchy depletion with residual, sparsely stained fibers. Five weeks after cuprizone withdrawal (remyelination), LFB intensity increased relative to the demyelinated state in both CC-M and CC-L (Fig. 2E–F), but the myelin band remained thinner and more heterogenous than in controls, indicating incomplete structural restoration.

Quantitative analysis of LFB intensity corroborated the morphological observations. Across the whole CC, mean LFB intensity was highest in controls, decreased significantly following cuprizone treatment (lowest in the demyelination group), and increased during remyelination to values that did not differ significantly from control. The Kruskal–Wallis test showed a highly significant group effect for the whole CC ($p < 0.0001$). Post-hoc comparisons indicated significant differences between control and demyelination ($p < 0.0001$) and between demyelination and remyelination ($p < 0.0001$), whereas control versus remyelination did not differ significantly ($p > 0.05$).

Subregional analysis revealed the same overall pattern in CC-M and CC-L (Kruskal–Wallis, $p < 0.0001$ for each). Notably, a significant difference between CC-L and CC-M was observed only in the demyelination group: LFB intensity in CC-L was lower than in CC-M ($p = 0.03$). In both the control and remyelination groups the medial and lateral subregions showed similar LFB intensities (control: no significant difference; remyelination: CC-M slightly higher than CC-L but not statistically significant, $p > 0.05$). Collectively, these data indicate pronounced myelin loss after cuprizone exposure – with greater vulnerability of the lateral CC during demyelination – and substantial, though incomplete, recovery of LFB-detectable myelin following treatment withdrawal.

DISCUSSION

Our findings demonstrate that cuprizone administration with water induces a robust, regionally heterogeneous, and reversible demyelination of the CC in C57BL/6 mice. LFB staining revealed a marked reduction in myelin signal after five weeks of cuprizone exposure, with greater depletion in the CC-L than in the CC-M. Following five weeks of recovery, LFB intensity increased in both subregions to levels that were not statistically different from controls; however,

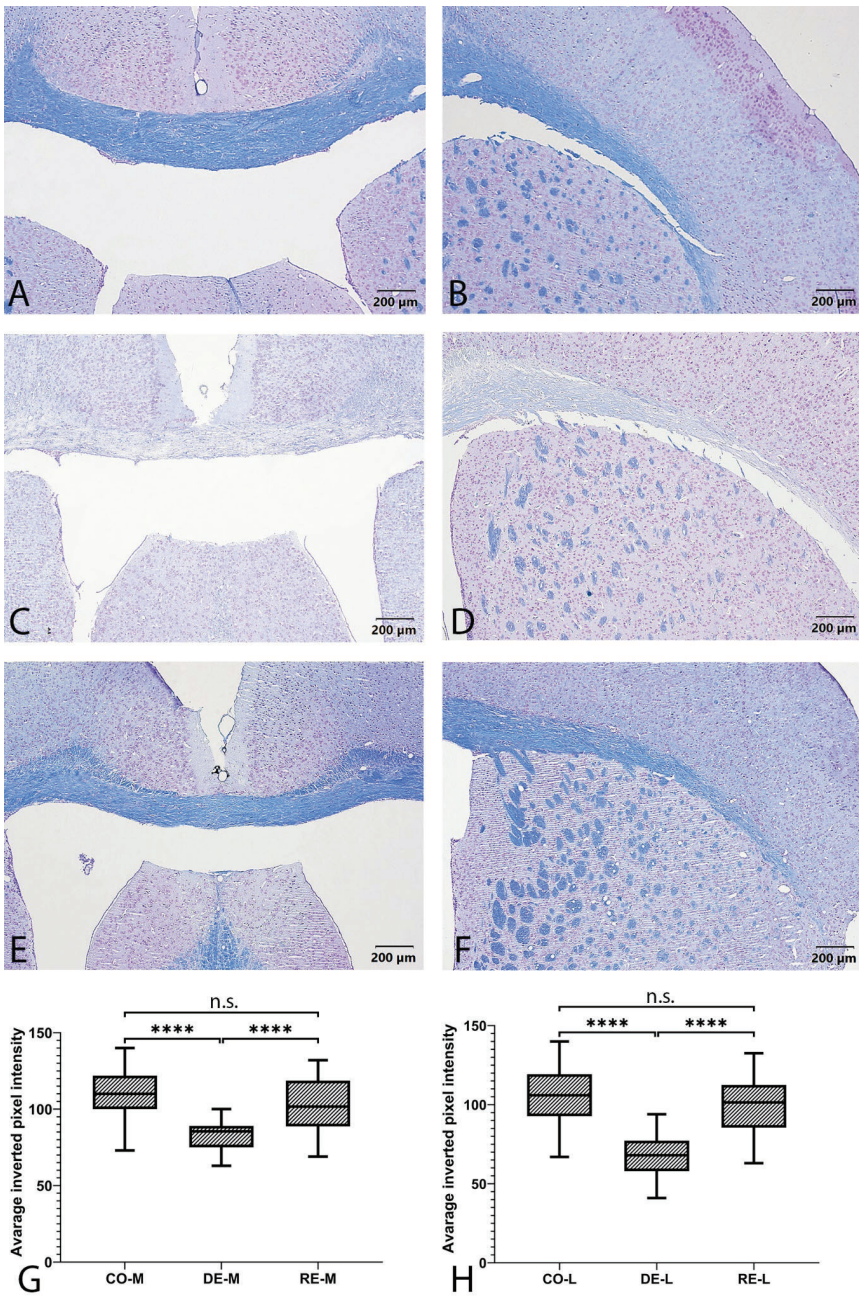

Fig. 2. Luxol Fast Blue (LFB)/Cresyl violet staining of coronal mouse brain sections highlighting myelin within the corpus callosum (CC). Panels are arranged by experimental condition and subregion: **A–B**, control; **C–D**, demyelination (DE); **E–F**, remyelination (RE). Within each pair, A, C, E = medial corpus callosum (CC-M); B, D, F = lateral corpus callosum (CC-L). Scale bar = 200 µm in all panels. (G) Quantification of LFB signal in the medial CC (CO-M, DE-M, RE-M) presented as box-and-whisker plots of average inverted pixel intensity (higher values indicate greater myelin content); (H) corresponding quantification for the lateral CC (CO-L, DE-L, RE-L). Data are derived from n = 150 visual fields per group. Boxes indicate the interquartile range with the median; whiskers denote minimum and maximum values. Statistical comparisons were made by Kruskal–Wallis with post-hoc testing; **** $p < 0.0001$, n.s. = not significant ($p > 0.05$)

the myelin band remained thinner and more heterogeneous than in the untreated CC, indicating incomplete structural restoration. Thus, our results demonstrate pronounced myelin loss during cuprizone exposure, regional susceptibility within the CC, and substantial – but morphologically incomplete – remyelination after toxin withdrawal. The absence of a statistically significant difference between the control and recovery groups further supports the capacity of the adult brain to restore myelin content once the toxin has been removed.

Our results are consistent with previous studies describing cuprizone-induced demyelination as a dynamic and spatially heterogene ous process. Toomay et al. reported that cuprizone reduces myelin content in both rostral and caudal regions of the CC, although significant effects were primarily detected in caudal regions and were strongly dependent on the formulation of the toxin [13]. The heightened vulnerability of the caudal CC described in their study corresponds well with our observation of pronounced demyelination followed by recovery, supporting the concept that regional susceptibility and exposure kinetics jointly determine the severity of myelin loss [13]. Their findings further suggest that demyelination is influenced not only by toxin presence, but also by effective bioavailability and regional metabolic sensitivity, emphasizing the importance of strict experimental control when modeling demyelination [13].

Our data also align with the anatomical patterns described by Hibbits et al., who showed that the CC and hippocampal fiber tracts undergo marked demyelin-

ation after prolonged cuprizone exposure, whereas the cerebellum remains largely unaffected [14]. This regional selectivity supports the interpretation that cuprizone does not act as a generalized neurotoxin but preferentially targets specific oligodendrocyte populations and microenvironments. The remyelination we observed in the CC after cuprizone withdrawal mirrors the spontaneous repair described by Hibbits et al., highlighting the intrinsic regenerative capacity of this white matter tract [14]. Steelman et al. further demonstrated that cuprizone-induced demyelination is spatially polarized, with caudal structures, such as the splenium and dorsal hippocampal commissure, showing near-complete myelin loss, while more rostral regions are relatively spared [15]. Their observation of lipid debris accumulation and subsequent clearance provides a mechanistic basis for the reversible LFB changes observed in our study, suggesting that normalization of staining reflects both new myelin synthesis and efficient removal of degraded myelin. In addition, Schmidt et al. showed that demyelination follows defined rostro-caudal and medio-lateral gradients, rather than occur uniformly across the CC [16]. This spatial heterogeneity implies that whole-structure measurements, such as those used here, integrate multiple subregional processes and may therefore mask subtle residual differences at the subregional level [16].

The validity of LFB as a marker of myelin content is further supported by imaging–histology correlation studies. Tagge et al. demonstrated a strong relationship between histological myelin loss and changes in magnetization transfer ratio (ΔMTR), validating the use of myelin-sensitive markers as reliable indicators of demyelination and remye lination [17]. Similarly, Fjær et al. showed that MTR and proteolipid protein (PLP) changes evolve with distinct temporal and regional patterns, reinforcing the concept that demyelination and repair follow anatomically and temporally specific trajectories [18].

Genetic background also influences susceptibility to demyelination and the efficiency of remyelination. Studies using Black Gold staining have shown strain-dependent differences in demyelination severity and repair capacity [19-21]. Genetic background is a critical determinant of susceptibility to cuprizone-induced pathology. C57BL/6 mice exhibit significantly greater sensitivity to cuprizone than CD1 (outbred white) mice, developing rapid and pronounced demyelination of the corpus callosum within approximately four weeks of treatment [19]. In contrast, CD1 mice display delayed and attenuated demyelination even after prolonged exposure, retain higher numbers of mature oligodendrocytes, and show weaker activation of glial and progenitor cell populations, indicating relative resistance to cuprizone toxicity [19]. Consequently, C57BL/6 mice are widely regarded as the preferred strain for cuprizone-based studies because they provide faster, stronger, and more reproducible demyelination, thereby enhancing experimental sensitivity and reproducibility [19]. Although strain effects were not directly examined in the present study, these findings may contribute to variability across experiments and highlight the importance of biological context when interpreting cuprizone models.

Finally, Wergeland et al. demonstrated that CC demyelination occurs rapidly, stabilizes, and is followed by remyelination after cuprizone withdrawal, whereas cortical regions may exhibit incomplete recovery [22]. This temporal profile closely parallels our observation of reversible CC demyelination and supports the view that the CC is both highly vulnerable to injury and highly capable of repair [22].

LIMITATIONS

While LFB staining provides a sensitive and well-established histochemical measure of myelin content, it has important limitations. LFB intensity reflects gross myelin abundance but does not resolve ultrastructural features, such as myelin thickness, internodal length, nodal organization, or axonal integrity. Consequently, normalization of LFB signal after cuprizone withdrawal should not be interpreted as proof of complete structural or functional recovery. To determine whether remyelination restores normal myelin architecture and conduction, complementary analyses are required: electron microscopy to assess g-ratio and internodal structure, immunohistochemistry for axonal and nodal markers, and electrophysiological measurements to test conduction velocity. Moreover, biochemical or imaging measures that distinguish newly formed versus residual/compacted myelin would strengthen conclusions about the quality of repair.

CONCLUSION

In summary, five weeks of cuprizone exposure produced pronounced and regionally heterogenous demyelination of the mouse corpus callosum, with the lateral subregion showing greater vulnerability than the medial portion, as demonstrated by both morphological Luxol Fast Blue staining and quantitative analysis. Withdrawal of cuprizone for five weeks led to a significant recovery of LFB-detectable myelin, such that whole–corpus callosum values were no longer different from controls, indicating a strong intrinsic capac-

ity for remyelination. However, the persistently thinner and more heterogenous myelin bands observed after recovery show that this repair was structurally incomplete despite normalization of mean staining intensity. Together, these findings highlight both the sensitivity of the corpus callosum to toxin-induced demyelination and its ability to undergo substantial spontaneous remyelination, while emphasizing the importance of region-specific and multimodal analyses to accurately assess the quality of myelin repair.

Author Contributions: *Conceptualization, L.G.; methodology, L.G.; validation, L.G., B.L. and G.P.G.; formal analysis, L.G. and K.P.; writing – original draft preparation, L.G. and K.P.; writing – review and editing, B.L. and G.P.G.; visualization, L.G.; supervision, G.P.G. and B.L. All authors have read and agreed to the published version of the manuscript.*

Funding: *This study is financed by the European Union-NextGenerationEU, through the National Recovery and Resilience Plan of the Republic of Bulgaria, project BG-RRP-2.004-0004-C01 Strategic research and innovation program for development of Medical University – Sofia.*

Institutional Review Board Statement: *All interventions conformed to Directive 2010/63/EU on the protection of animals used for scientific purposes and were approved by the Bulgarian Food Safety Agency (Approval Protocol No. 416/19.12.2024).*

Data Availability Statement: *The raw data supporting the conclusions of this article will be made available by the authors upon request.*

Conflicts of Interest: *The authors declare no conflicts of interest.*

REFERENCES

1. Gean-Marton AD, Vezina LG, Marton KI, et al. Abnormal corpus callosum: a sensitive and specific indicator of multiple sclerosis. Radiology, 1991, 180(1):215-21. doi: 10.1148/radiology.180.1.2052698.
2. Seitaridou Y, Dimitrova M, Chamova T, et al. Cost-effectiveness of multiple sclerosis therapies – a literature review. Acta Med Bulg, 2022, 49(4):69-80. doi: 10.2478/amb-2022-0046.
3. Lindner M, Heine S, Haastert K, et al. Sequential myelin protein expression during remyelination reveals fast and efficient repair after central nervous system demyelination. Neuropathol Appl Neurobiol, 2008, 34:105–114. doi: 10.1111/j.1365-2990.2007.00879.x.
4. Matsushima GK, Morell P. The neurotoxicant, cuprizone, as a model to study demyelination and remyelination in the central nervous system. Brain Pathol, 2001, 11:107–116. doi: 10.1111/j.1750-3639.2001.tb00385.x.
5. Kipp M. How to use the cuprizone model to study de- and remyelination. Int J Mol Sci, 2024, 25:1445. doi: 10.3390/ijms25031445.
6. Hiremath MM, Saito Y, Knapp GW, et al. Microglial/macrophage accumulation during cuprizone-induced demyelination in C57BL/6 mice. J Neuroimmunol, 1998, 1:38–49. doi: 10.1016/S0165-5728(98)00168-4.
7. Gharagozloo M, Mace JW, Calabresi PA. Animal models to investigate the effects of inflammation on remyelination in multiple sclerosis. Front Mol Neurosci, 2022, 15:995477. doi: 10.3389/fnmol.2022.995477.
8. Morgan ML, Teo W, Hernandez Y, et al. Cuprizone-induced Demyelination in Mouse Brain is not due to Depletion of Copper. ASN Neuro, 2022, 14:17590914221126367. doi: 10.1177/17590914221126367.
9. Landzhov B, Gaydarski L, Stanchev S, et al. A Morphological and behavioral study of demyelination and remyelination in the cuprizone model: Insights into APLNR and NG2+ cell dynamics. Int J Mol Sci, 2024, 25(23):13011. doi: 10.3390/ijms252313011.
10. Buonvicino D, Ranieri G, Chiarugi A. Cuprizone-dependent De/Remyelination responses and functional correlates in mouse strains adopted to model relapsing, chronic and progressive experimental autoimmune encephalomyelitis. Neurotox Res, 2021, 39(3):658-666. doi: 10.1007/s12640-021-00331-3.
11. Lindner M, Fokuhl J, Linsmeier F, et al. Chronic toxic demyelination in the central nervous system leads to axonal damage despite remyelination. Neurosci Lett, 2009, 453(2):120-5. doi: 10.1016/j.neulet.2009.02.004.
12. Paxinos G, Franklin K. The mouse brain in stereotaxic coordinates. 2nd ed. Academic Press. Cambridge, MA, USA, 2001, 55–63.
13. Toomey LM, Papini M, Lins B, et al. Cuprizone feed formulation influences the extent of demyelinating disease pathology. Sci Rep, 2021, 11(1):22594. doi: 10.1038/s41598-021-01963-3.
14. Hibbits N, Pannu R, Wu TJ, Armstrong RC. Cuprizone demyelination of the corpus callosum in mice correlates with altered social interaction and impaired bilateral sensorimotor coordination. ASN Neuro, 2009, 1(3):e00013. doi: 10.1042/AN20090032.
15. Steelman AJ, Thompson JP, Li J. Demyelination and remyelination in anatomically distinct regions of the corpus callosum following cuprizone intoxication. Neurosci Res, 2012, 72(1):32-42. doi: 10.1016/j.neures.2011.10.002.
16. Schmidt T, Awad H, Slowik A, et al. Regional heterogeneity of cuprizone-induced demyelination: topographical aspects of the midline of the corpus callosum. J Mol Neurosci, 2013, 49(1):80-8. doi: 10.1007/s12031-012-9896-0.
17. Tagge I, O'Connor A, Chaudhary P, et al. Spatio-temporal patterns of demyelination and remyelination in the cuprizone mouse model. PLoS One, 2016, 11(4):e0152480. doi: 10.1371/journal.pone.0152480.
18. Fjær S, Bø L, Lundervold A, et al. Deep gray matter demyelination detected by magnetization transfer ratio in the cuprizone model. PLoS One, 2013, 8(12):e84162. doi: 10.1371/journal.pone.0084162. Erratum in: PLoS One. 2014;9(10):e111828.
19. Yu Q, Hui R, Park J, et al. Strain differences in cuprizone induced demyelination. Cell Biosci, 2017, 7:59. doi: 10.1186/s13578-017-0181-3.
20. Savaskan NE, Weinmann O, Heimrich B, Eyupoglu IY. High resolution neurochemical gold staining method for myelin in peripheral and central nervous system at the light- and electron-microscopic level. Cell Tissue Res, 2009, 337(2):213-21. doi: 10.1007/s00441-009-0815-9.
21. Emery B. Regulation of oligodendrocyte differentiation and myelination. Science, 2010, 330(6005):779-82. doi: 10.1126/science.1190927.
22. Wergeland S, Torkildsen Ø, Myhr KM, Mørk SJ, Bø L. The cuprizone model: regional heterogeneity of pathology. APMIS. 2012 Aug;120(8):648-57. doi: 10.1111/j.1600-0463.2012.02882.x.